Adaptive Optics Reconstruction Utilizing Super-Sampled Deformable Mirror Influence Functions

David Redding, Scott Basinger, Gary Brack, Richard Dekany
Jet Propulsion Laboratory, California Institute of Technology

Ben Oppenheimer
California Institute of Technology

ABSTRACT

Control laws for an adaptive optics system for the Palomar Mountain Hale Telescope are described. These are derived using a linear matrix model of the optics, which gives the Hartman-sensor centroids and the science camera wavefront error as a function of deformable mirror actuation and induced atmospheric phase. The matrices defining this system are measured from the AO optics directly. Deformable mirror influence functions are calibrated at finer spatial resolution than the wavefront sensor can resolve. A minimum-wavefront compensator exploits this information to achieve better performance than a centroid-nulling approach, at the cost of more real-time computation. Gains for the compensator can be updated using Kalman filtering techniques to track the evolution of the atmospheric covariance matrix.

1.INTRODUCTION

This paper describes adaptive optics control laws that are now being implemented on the Palomar Mountain Hale telescope. This system uses a Shack-Hartman sensor observing natural guide stars to drive a 241 active-actuator deformable mirror and a fast steering mirror. A full description of this system is provided in Ref. 1. First closed-loop results are expected in March 1998 using a centroid-nulling controller, and in May 1998 using the minimum-wavefront compensator described here.

The heart of the AO system is its controller. This is implemented in 3 stages, as sketched in Fig. 1. The first stage processes the raw CCD outputs to determine Hartman cell centroids. This "centroider" uses a 2-stage filter, with gains updated according to guide-star and seeing characteristics, to approach quad-cell accuracy in a 4-by-4-pixel format. The centroiding is described in detail in Ref. 2.

The second stage of the controller takes the centroids and determines commands for the deformable mirror (DM) and fast-steering mirror (FSM). This "reconstructor," so called because it reconstructs the aberrated wavefront from the centroid signal prior to computing the actuator commands, is the main topic of this paper. Like the centroider, the reconstructor uses gains and other factors that are updated periodically to optimize performance with respect to seeing and guide-star properties.

The reconstructor includes a Kalman filter [4], which estimates the wavefront at every controller time step, using gains that balance the uncertainty in the current WFS measurement against error in the prior wavefront estimate. The control law implemented in the reconstructor balances uncertainty in the estimate of the wavefront against actuation error to minimize the RMS wavefront error (WFE) in the current time slice. The combination of the estimator and controller is a classical optimal compensator. Evolution of the compensator gains is driven by the error history of the compensator, providing a self-correcting capability through the Kalman filter update equations.

The final stage is a digital filter, used to temporally smooth inputs to the DM and to improve low-frequency accuracy. The entire AO loop runs at 500 Hz, to achieve a closed-loop bandwidth approaching 60 Hz. Controller gains are updated, following calibration of the optics, and during observation runs, based on wavefront sensor measurements. The new gains are computed at appropriate intervals by "matrix generating software" (MGS), which runs off-line in an engineering workstation-class computer.

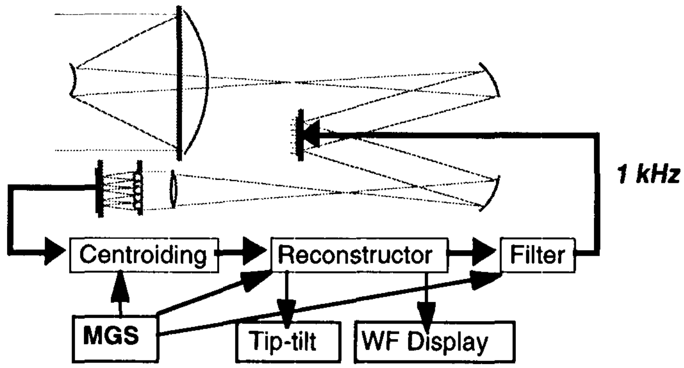

Figure 1. Controller signal flow.

The discussion in this paper begins by defining the plant to be controlled, in the form of two linear matrix equations. Deformable mirror and other component characteristics are reviewed. Two distinct control approaches are then developed. The first is a "centroid nulling" controller, which seeks to minimize centroid errors and is implemented using a single matrix multiply. The second is the Kalman-filter based wavefront-nulling reconstructor; its implementation is slightly more complex, as it requires 2 matrix multiplies and a vector add. The excess processing, however, takes place largely during dead time, in preparation for the next computing cycle.

Examples are worked through using both approaches, showing that the minimum-wavefront control is the superior performer. It is shown that driving the centroids to null does not necessarily produce minimum wavefront error. Conversely, the minimum-wavefront solution often leaves non-null centroids. Evolution of the reconstructor gains is discussed, and the paper concludes with a review of the implentation of the controller in hardware.

2.AO SYSTEM REPRESENTATION

This section introduces a linear matrix modeling approach for Hartman-sensor based adaptive optics systems. The model includes separate equations for the WFS centroids and the exit pupil wavefront, in contrast to the usual approach of treating the centroids as the spatial derivatives of the wavefront.

For ease in visualization, let us first consider an example AO system consisting of only 6-by-6 Hartman cells, centered (nearly) in a rectangular pupil, onto which is mapped a DM with a 7-by-7 actuator array. This pupil is illustrated by Fig. 2, where actuators are indicated by hollow dots; the WFS cells are formed with the actuators at each corner. Spacing of the actuators on the pupil is 100 cm. The smaller solid dots are the points where the wavefront is evaluated. These over-sample the pupil compared to the WFS cells, allowing resolution of higher spatial frequency effects than can be seen in the WFS.

The optics assumed for this example are a simplified representation of the Palomar AO system, with a large telescope feeding an off-axis parabola, which reimages the primary mirror onto the deformable mirror (Fig. 3). The DM implements the higher-order corrections. A second off-axis parabola refocusses the beam, which is then split to send light into both a science imaging camera and into the Hartman wavefront sensor (WFS). Within the WFS, a lens creates a second pupil image at a lenslet array. The resulting spot array is focussed on a CCD array, with each spot nominally aligned at the center of a 4-by-4 pixel subarray. A FSM is located between the DM and the telescope to implement tilt corrections.

The atmospheric state equation, governing the transition of the atmospheric phase from one time step (denoted by a subscript i) to the next is given by:

$$a_{i+1} = a_i + \lambda_i \tag{1}$$

The a_i states are the phases of the wavefront at the entrance pupil of the telescope, as sketched in Fig. 3, at time step i, sampled at the small solid dots indicated in Fig. 2. The mean of ai is zero, and the covariance at a given instant of time is A_i. A_i can reasonably be generated assuming Kolmogorov turbulence, as a function of r0. As shown in Fig. 2, the ai oversample the WFS cells by a factor of m = 4. The dimension of $\boldsymbol{a_i}$ is thus m^2n^2 or 625 for the example. The matrix dc/da thus has dimension 72-by-625.

The time evolution of the atmosphere is here treated as a noise process, driven by the vector λ_i with covariance Λ_i.

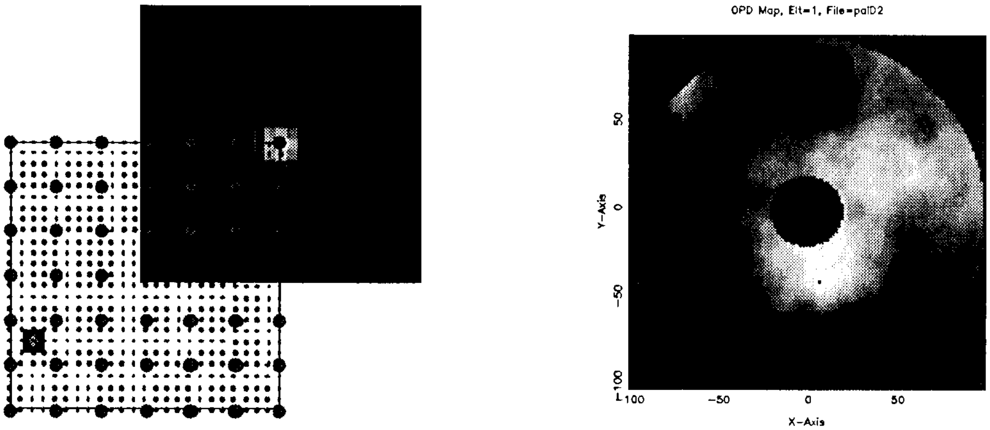

Figure 2. Pupil diagram showing DM influence function and wavefront state sampling; typical realization of atmospheric phase for Palomar AO.

The measurement equation captures the influence of the DM and atmospheric phase errors on the Hartman centroids. At the instant of the centroid measurement, at the start of a new control cycle:

$$c_i = \frac{dc}{da}a_i + \frac{dc}{du}(u_{i-1} + q_{i-1}) + r_i \tag{2}$$

Here $\boldsymbol{c_i}$ is a vector of dimension 72 containing the x- and y-centroids for each of the 36 subapertures, at time ti. The DM actuator commands that were applied in the previous time step are in the $\boldsymbol{u_{i-1}}$ vector, which is of dimension 49. The $\boldsymbol{q_{i-1}}$ vector contains actuation noise terms, with covariance Q_i. Actuation noise captures gain calibration errors.

The sensitivity of the centroids to DM actuators – the matrix dc/du – can be measured easily by pushing actuators and recording the centroid signals that result, then dividing by the amount pushed. With idealized actuators, the result of pushinga single actuator is to shift the centroid of the 4 immediately adjacent Hartman cells directly away from the actuator, at 45° to the grid layout. Actual hardware produces more complication, coupling the response over 36 or more adjacent WFS cells, causing actuator scale factor and alignment problems, etc.

The $\boldsymbol{r_i}$ vector contains 72 centroid measurement error elements, which are driven by detection noise as processed by the centroider 2-stage filter. These are assumed to be zero-mean and uncorrelated, with a standard deviation set by sensor and filter characteristics determined chiefly by subaperture SNR.

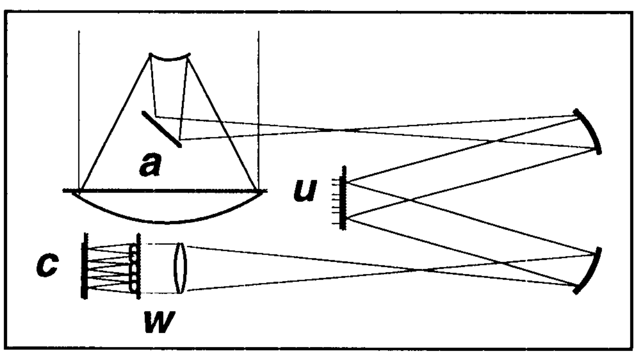

Figure 3. Optics layout for Palomar AO (left) and example problem (right).

The third equation models the influence of the DM and atmosphere on the WFS and science camera wavefront, represented by a vector w_i. It is the objective of the AO system to drive this to zero. The wavefront equation takes the form:

$$w_i = \frac{dw}{da}a_i + \frac{dw}{du}(u_{i-1} + q_{i-1}) \tag{3}$$

The wavefront vector w_i corresponds to the optical pathlengths of rays originating at the entrance pupil at the locations of the elements of a_i, (the small solid dots in Fig. 2) and then traced to the exit pupil located in the WFS or science camera. It has the same dimension of m2n2-by-1, or 625-by-1 in our example. The sensitivity of the wavefront with respect to the atmospheric states, dw/da, is nominally an identity matrix of size 625-by-625. Deviations occur due to imperfections in the AO and telescope system optics, but these can be calibrated accurately.

The sensitivity of the wavefront to DM actuations, given in matrix dw/du, records the influence function of each actuator at the m-times higher spatial scale of a_i and w_i. It is measured directly, using an interferometer looking back through the AO system at a point source located at the paraxial focus of the telescope. The DM actuators are pushed in turn, the WF recorded and normalized as before.

Influence functions have been measured for the Xintetics 349-actuator.[3] For our model we are using an "average" actuator. As shown in Figs. 2 and 4 , each actuator produces a significant response for a radius of about 2 actuator spacings, pushing up and down by amounts that decrease with increasing distance from the actuator. There is significant curvature to the response that is not resolved at the WFS cell scale, but is captured by the m-times finer sampling provided by w_i.

The validity of this model depends on accurate measurement of the various component matrices. Other effects such as anisoplatism and scintillation are not modelled. Nonlinearity effects, model range-of-validity considerations (with respect to changes in the optics in particular) and other factors are not addressed here. These effects reduce absolute performance for the approaches considered here, but are not expected to change the relative performance.

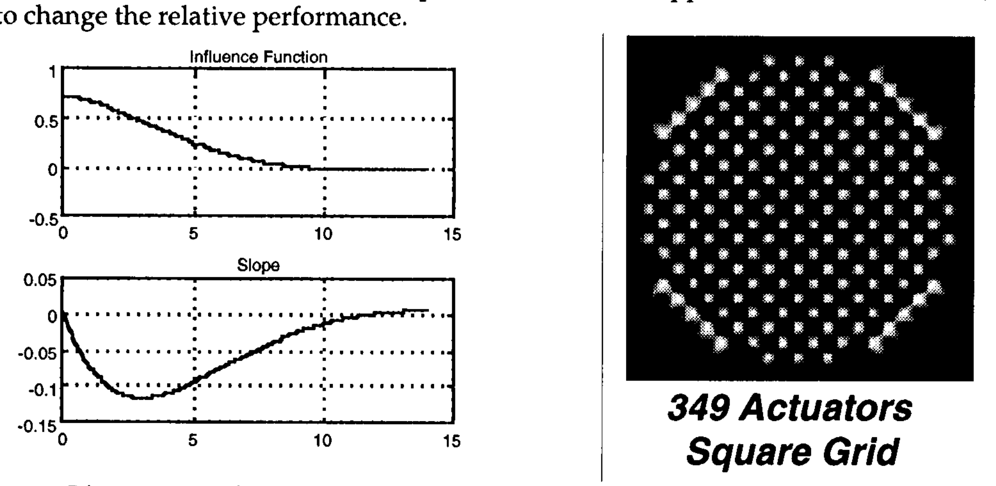

Figure 4. DM influence function; waffle mode for Palomar AO format DM.

3.CENTROID-NULLING CONTROLLER

Several other practitioners have proposed or implemented controllers that use measured sensitivity matrices in control laws that seek to minimize centroid error.[5,6] For sake of comparison with the Palomar minimum-wavefront approach, we formulate a centroid controller here. This discussion is simplified and not intended to duplicate any particular group's approach.

The assumption underlying the centroid controller is that the centroids c_i represent the gradient of w_i in the WFS, and that driving c_i to zero will also flatten the wavefront w_i. This approach is fundamentally limited to WFS resolution limits in its response: knowledge of the influence functions dw/du at the finer scale are not used. No attempt is made to separate the part of w_i due to a_i from that due to u_i. The centroid controller does not explicitly utilize prior knowledge of the wavefront. It does not exploit knowledge of the statistics of the atmosphere or of the measurement and actuation errors. It does have a simple implementation in the real-time computer, however.

The centroid control problem is to minimize:

$$J_{cent} = \frac{1}{2}c_i^T c_i \tag{4}$$

subject to the constraint of Eqn. 2. The solution is straight-forward:

$$u_i = -\left(\frac{dc}{du}\right)^+ c_i = -G_c c_i \tag{5}$$

Here the gain matrix Gc is of dimension nu-by-nc. The centroid and wavefront residuals following a single control step are:

$$\delta c_i = c_i + \frac{dc}{du}(u_i + q_i) \tag{6}$$

$$\delta w_i = w_i + \frac{dw}{du}(u_i + q_i) \tag{7}$$

4.MINIMUM-WAVEFRONT CONTROLLER

The minimum-wavefront reconstructor differs from the centroid-nulling controller of the previous section in several respects. It is explicitly designed to minimize the WFS exit pupil wavefront error. It utilizes the finer resolution of the measured dw/du influence functions to extend the resolution of the DM-related component of WFE beyond the WFS resolution limit. It makes use of prior knowledge of the wavefront, as well as knowledge of the statistics of the atmosphere and of the measurement and actuation errors to optimally filter the measurements in applying the control. This increased versatility results in improved performance. It comes at the cost of a more complex implementation in the real-time computer, however.

Conceptually, the wavefront controller operates in 2 stages at each time step. The first stage explicitly estimates the wavefront a_i at the entrance pupil of the telescope, given the current centroid measurements, the previous DM actuation commands, and the previous estimate $\bar{a}_{i-1}$ which is now about 1 msec old. The second stage takes the estimate $\bar{a}_i$ and computes the actuator commands u_i. Periodic updates of the covariance of the atmospheric states are performed to keep the gains current.

Actual implementation differs from this picture slightly, as discussed below. There is no actual evaluation of $\bar{a}_i$ in the on-line processing. The computation of the control is split so that part is done in preparation for the next time step, rather than all being done after the receipt of the centroid data. The latter significantly speeds computation of the control, so that the time from receipt of data to actuation of the DM is commensurate with the time for the centroid-nulling controller.

It is convenient to rewrite the measurement equation to lump together the noise terms, namely the measurement noise r and the actuation noise q_i (which represents the uncertainty in the knowledge of the DM state provided by u_i):

$$c_i = \frac{dc}{da}a_i + \frac{dc}{du}u_{i-1} + r_{ci} \tag{8}$$

The combined noise terms r_c have covariance R_c, where:

$$r_{ci} = \frac{dc}{du}q_i + r_i \tag{9}$$

$$R_c = \frac{dc}{du}Q\left(\frac{dc}{du}\right)^T + R \tag{10}$$

The estimation problem is to determine a_i , given centroid measurements c_i corrupted by noise r_i with covariance R, and given known previous actuator commands u_{i-1} corrupted by noise q_{i-1} with covariance Q. The estimated covariance for the atmospheric states a_i is A, which is assumed to be defined initially by the Kolmogorov structure function, and which can updated based on off-line computations.

A very reasonable estimate is provided by the minimum-variance estimator, which seeks to balance the uncertainty in the estimate across the sources of that uncertainty. The cost function Jest is minimized:

$$J_{est} = \frac{1}{2}\left[\bar{a}_i^T A^{-1}\bar{a}_i + \left(c_i - \frac{dc}{da}\bar{a}_i - \frac{dc}{du}u_{i-1}\right)^T R^{-1}\left(c_i - \frac{dc}{da}\bar{a}_i - \frac{dc}{du}u_{i-1}\right)\right] \tag{11}$$

J_{est} has a minimum at:

$$\delta J_{est} = 0 = \delta\bar{a}_i^T\left[A^{-1}\bar{a}_i + \left(\frac{dc}{da}\right)^T R^{-1}\left(c_i - \frac{dc}{da}\bar{a}_i - \frac{dc}{du}u_{i-1}\right)\right] \tag{12}$$

The nontrivial solution for the estimate is:

$$\bar{a}_i = K\left(c_i - \frac{dc}{du}u_{i-1}\right) \tag{13}$$

The matrix K is the estimator gain matrix:

$$K = E^{-1}\left(\frac{dc}{da}\right)^T R^{-1} \tag{14}$$

Here E is the covariance of the estimate error residuals:

$$E^{-1} = A^{-1} + \left(\frac{dc}{da}\right)^T R^{-1}\frac{dc}{da} \tag{15}$$

The dimension of K is na-by-nc, where na grows with the oversampling factor m.

The controller phase of the compensator takes the estimated wavefront and generates commands u_i. The control objective function, to be minimized, is J_{con}:

$$J_{con} = \frac{1}{2}w_i^T w_i \tag{16}$$

The resulting control is computed as:

$$u_i = \left(\frac{dw}{du}\right)^+ \frac{dw}{da}\bar{a}_i = -G\bar{a}_i \tag{17}$$

The controller gain matrix G has dimension nu-by-na, where na is increased by the oversampling factor. The total compensator, created by using the estimates $\bar{a}_i$ to drive the control computation, is:

$$u_i = -GK\left(c_i - \frac{dc}{du}u_{i-1}\right) \tag{18}$$

This is rewritten in terms of 2 gain matrices G_c and G_u:

$$u_i = -G_c c_i - G_u u_{i-1} \tag{19}$$

$$G_c = -GK \tag{20}$$

$$G_u = -GK\frac{dc}{du} \tag{21}$$

The dimension of G_c is nu-by-nc and that of G_u is nu-by-nu. Neither matrix size is increased by the oversampling factor m. The second product of Eq. 19 can be pre-computed following determination of u_{i-1}, so the computational burden following measurement of the ci is essentially the same as that for the centroid-nulling controller (Eq. 5). The wavefront residuals and the covariance of the residuals are:

$$\delta w_i = w_i + \frac{dw}{du}(u_i + q_i) \tag{22}$$

(23)

5.KALMAN FILTER ESTIMATOR

A more elaborate (and computationally very intensive) approach to the estimation part of the minimum wavefront compensator is provided by the well-known Kalman filter.[4] This approach extends the minimum-variance estimator just described to update not just the state ai, but also its covariance A and the estimator gains K. It provides a means to use the measured centroids to improve knowledge of the atmosphere and so to tune the response of the compensator. It is too computationally intensive to implement in the real-time AO loop, but can be run off-line as part of the Matrix-Generating Software, to provide periodic updates to the K matrix. A sequence of centroids and DM actuator commands is recorded and then played back through the filter equations, to better estimate the evolving ai and A. The updated A is then uploaded into the real-time compensator.

The evolution of a_i between updates is given by Eq. 1. For the Kalman filter, the estimate of ai now is:

$$\bar{a}_i = \bar{a}_{i-1} + K_i\left(c_i - \frac{dc}{da}\bar{a}_i - \frac{dc}{du}u_i\right) \tag{24}$$

The compensator uses gains Ki producing estimates with error Ei:

$$K_i = E_i\left(\frac{dc}{da}\right)^T R_c^{-1} \tag{25}$$

$$E_i = \left[A_i^{-1} + \left(\frac{dc}{da}\right)^T R_c^{-1}\frac{dc}{da}\right]^{-1} \tag{26}$$

A new value for A is thus:

$$A_{i+1} = E_i + \Lambda \tag{27}$$

Various filtering and smoothing methods exist that offer potential in making best use of the available information. We will be experimenting with these approaches.

6.EXAMPLE RESULTS

Comparison of the performance of the centroid-nulling and wavefront controllers reveals some interesting differences. The 6-by-6 example introduced above was used, with the WFS cell size set to 100 cm. Random realizations of the atmosphere were generated, using Kolmogorov statistics driven by r_0. Atmospheric covariance A was determined from the Kolmogorov generating function, also driven by r_0. Three typical realizations at 3 values of r_0 are shown in Fig. 5. In each case, the upper third of the frame shows the raw phase disturbance, the middle third of each frame shows the wavefront compensated by the centroid control, and the bottom third shows the effect of the minimum-wavefront control.

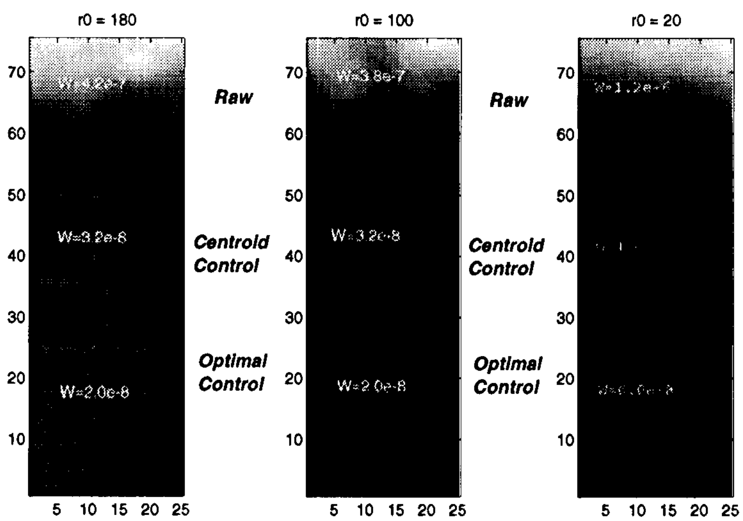

Figure 5. Example results: 3 realizations at 3 values of r_0.

In all cases, the minimum-wavefront control produces lower wavefront error than the centroid-nulling control. In the poor seeing case (r_0 = 20 cm) the centroid-nulling control shows significant waffle mode. This is not seen in the minimum-wavefront controller. By over-sampling the wavefront compared to the WFS sampling, the minimum-wavefront controller builds in many additional points of constraint. The waffle mode, which is not observable in the centroid measurements, *is* observable in the DM actuation contribution to the wavefront estimate, and so is suppressed by the compensator. This will always be the case unless the atmospheric covariance matrix A becomes dominated by a waffle mode, which is not expected in nature.

Results accumulated using Monte Carlo simulation for the same system show some interesting trends. As seen in Fig. 6, the minimum-wavefront controller significantly outperforms the centroid-nulling controller in WFE, and significantly underperforms it in centroid error. This is because the minimum wavefront condition occurs with a finite centroid offset. This distinction leads directly to the difference in performance observed here.

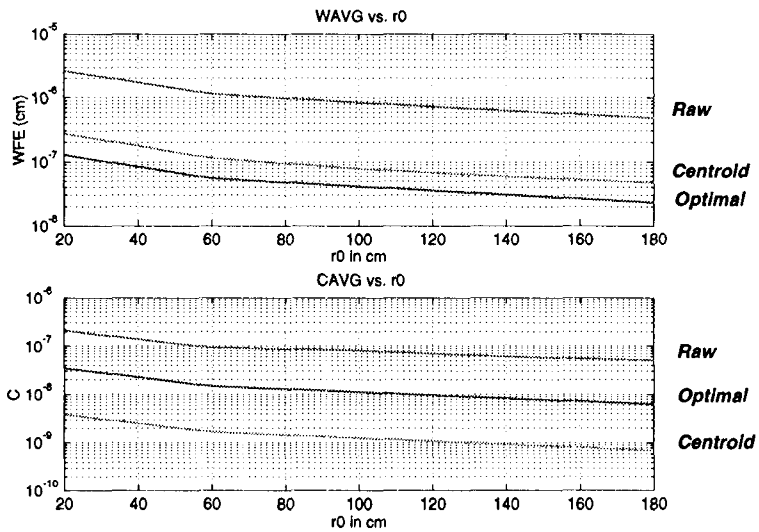

Figure 6. Example results: WF and centroid residuals vs. r_0, for 100 Monte Carlo trials/datapoint.

7.CONCLUSION

A linear model of an adaptive optics system, in the form of 2 matrix difference equations, has been used to derive 2 different adaptive optics controllers. A centroid-nulling controller is formulated to minimize centroid error, on the assumption that so doing also minimizes wavefront error. A minimum-wavefront controller uses the correlations between the atmospheric states, represented by the covariance matrix A, to interpolate the measurements to a finer grid than is actually sampled. It uses the calibrated DM influence functions dw/du to do the same for the DM part of the wavefront. It computes the next actuation to minimize WFE at all of these points taken together. The result is better performance than the centroid-nulling approach. The minimum-wavefront controller is being implemented on the Mt. Palomar Hale 5-meter telescope.

8.ACKNOWLEDGEMENT

This work was performed at the Jet Propulsion Laboratory, California Institute of Technology, under contract with NASA.

9.REFERENCES

1. R. Dekany, "The Palomar Adaptive Optics System," *OSA Technical Digest*, pp. 40-42 (1996).

2. S. Shaklan, "Two-Stage Centroiding Algorithm for Palomar Adaptive Optics," JPL Internal Memorandum, January 23, 1995.
3. B. Oppenheimer et al, "Investigating a Xinetics Deformable Mirror," SPIE 3126 (1977).
4. A.E. Bryson and Y.C. Ho, *Applied Optimal Control*, Hemisphere Press, 1975.
5. W. Wild, E.J. Kibblewhite and R. Vuilleumier, "Sparse Matrix Wave-front Estimators for Adaptive Optics Systems for Ground-Based Telescopes," Optics Letters, Vol. 20, No. 9, May 1995.
6. W.Wild, "Innovative Wavefront Estimators fo Zonal Adaptive Optics," SPIE 3126, pp. 278-287 (1977).